International Journal of Engineering Research & Technology (IJERT)
ISSN: 2278-0181
Vol. 6 Issue 04, April-2017

Effects of Rotational Speeds and Tool Pin Geometry on Microstructure and Mechanical Properties of Refilled Friction Stir Spot Welds of Similar AA2024-T3 Aluminum Alloy Sheets

Haidar Kamal Ibrahim [1]
Asst. Prof. Dr. Abdul Wahab Hassan Khuder [2]
[1], [2] Engineering Technical College-Baghdad,
Middle Technical University,
Baghdad, Iraq

Dr. Muhammed Abdul Sattar Muhammed [3]
[3] College of Engineering,
Nahrain University, Baghdad, Iraq

***Abstract*-Friction stir spot welding (FSSW) is a type of solid state joining processes, which was derived from the linear friction stir welding (FSW) as an alternative method for single-point joining processes like resistance spot welding and fastening. The main limitation of FSSW is the keyhole that remains at the center of the spot after welding process, which can be classified as a defect for the friction stir spot welding in its conventional method. In this work, a newly developed technique called friction stir spot welding with refilling by friction forming process (FSSW-FFP) was used to remove the keyhole from the conventional FSSW joints. Both of this new technique and conventional friction stir spot welding process were used to weld lap shear specimens of AA2024-T3 aluminum alloy sheets, thickness 2 mm, and the results were compared. Two types of tool pin geometry (straight cylindrical & triangular) and three rotational speeds (535, 980, and 1325) rpm were used to study the effect of these parameters on the mechanical and microstructural properties of friction stir spot welds. The keyhole was successfully refilled by the new refilling process. The tensile-shear test results showed that the refilled FSSW specimens are better than the specimens welded by the conventional FSSW process at all tool rotational speeds with using different tool pin profiles. The minimum tensile shear load obtained from the conventional friction stir spot welds was improved (to about 45%) by the refill FSSW process. Fracture modes under tensile shear tests were analyzed in detail using the scanning electron microscope (SEM). The variation of microhardness in different regions of the spot was evaluated.**

Keywords: AA2024-T3 Al alloy, Friction stir spot welding, Refill FSSW, FFTool, Weld strength

1. INTRODUCTION

The increasing demands for energy saving and weight reduction in automotive and aerospace industry has leads to necessity of replacing certain ferrous parts with lightweight alloys and advanced high strength steels (HSS). This interest has created the need to develop a reliable joining technology which can able to produce aluminum-steel dissimilar joints of high quality instead of conventional fusion welding processes, because of dissimilar joining of these materials by a traditional fusion welding is rather complicated and difficult due to their different chemical and physical properties, particularly the difference in melting temperatures [1, 2]. Aluminum alloys are difficult to be fusion welded due to the requirements of gas shielding of weld pool and removal of oxide layers before or during the welding process. In addition to these limitations, there are several weld defects associated with the conventional fusion welding of aluminum alloys, such as porosity, oxide inclusions, brittle solidification, distortion due to residual stresses, and liquation cracking in the weld region [3, 4]. These defects deteriorate the weld quality and mechanical properties of the welded joints.

Therefore, solid state welding processes, such as friction welding, friction stir welding, explosion welding, hot pressure welding, etc. were developed in order to overcome a variety of problems and weld defects related to melting and solidification in fusion welding of aluminum alloys [1,5]. Friction stir welding (FSW) is a solid state welding process that was invented by Wayne Thomas at The Welding Institute (TWI), United Kingdom, in 1991 [6], and has emerged as a welding technique used in high strength alloys (2XXX, 6XXX, and 7XXX series) for aerospace, automotive and marine applications [7]. During FSW, the maximum temperature of the welded plates is typically ranges from 70% to 90% of the melting temperature of the workpiece material, so that better mechanical properties and fewer weld defects of the weld zone are produced when compared with conventional fusion welding [8, 9, 10]. Based on the friction stir welding (FSW), the Mazda Corporation of Japan proposed a friction stir spot welding (FSSW) method in an attempt to transfer some of the advantages of FSW to spot welding. The FSSW can also be called as conventional FSSW, which has been firstly applied in the real production line for Mazda RX-8 hood and rear door panel in 2003 [11,12,13]. The conventional friction stir spot welding (CFSSW) consists of three phases: plunging, stirring, and retracting as shown in Figure 1.

International Journal of Engineering Research & Technology (IJERT)
ISSN: 2278-0181
Vol. 6 Issue 04, April-2017

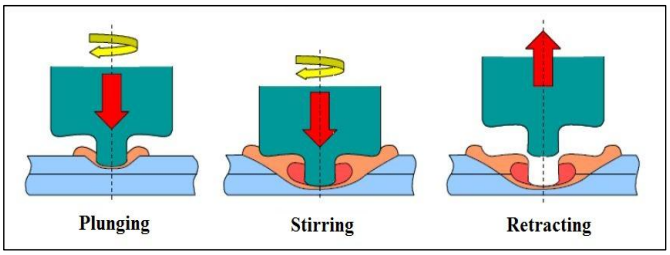

Figure 1: Schematic illustration of conventional FSSW process [14]

A non-consumable rotating tool is plunged into the overlapped workpieces that to be joined, hold for a certain duration time (dwell time) and finally retracted from the workpiece with no lateral movement or translation. The frictional heat generated at the tool-workpiece interface softens the surrounding materials. The rotational action and the downward force of the tool causes the material flow and mixing of the plasticized materials of upper and lower sheets result in the formation of a solid-state weld region [15,16,17,18]. One of the disadvantages of conventional friction stir spot welding is that a keyhole inevitably remains at the center of the weld nugget after tool retraction [19]. The keyhole acts as notch source causes stress concentration leads to crack propagation and subsequently weld failure under either monotonic or cyclic loading. Meanwhile, corrosion could take place preferentially at the bottom surface of the keyhole because of rainwater remains in the pin hole, where body paint hardly reaches the bottom [19, 20]. For these reasons, removal of the keyhole has attracted extensive attention of the researchers. Several techniques have been developed to remove the keyhole, such as the refill friction stir spot welding (RFSSW) using FSpW technique, the application of pinless rotating tools (Pinless FSSW), and ultrasonic spot welding (USW) [21,22,23].

Refill friction stir spot welding (FSpW) was invented by Helmholtz-Zentrum Geesthacht (GKSS) / Institute of Materials Research – Germany in 2004 [24,25]. By this process, keyhole is refilled with base material and no post-processes are need. Y. Uematsu et al [20] studied the refill friction stir spot welding (FSpW) of AA6061-T4 aluminum alloy sheets using a specially designed double-acting tool, which could refill the keyhole of the joints during the welding process. The results showed that the tensile-shear load of the welded joints with re-filled probe hole was improved to about (23%) at the optimum process conditions. However, the refilling process by FSpW method is sometimes fails to fully refill the plasticized material in the keyhole due to the inadequate flowing of materials [26, 27], thus weld imperfections such as incomplete refilling, no mixing, lack of mixing, and voids might appear in the refilled region [28, 29, 30], which have an important effect on the crack initiation when the joint is subjected to external loading. In addition to some of FSpW limitations which include the complicated procedure of welding machine and tool as well as higher cost [14].

In order to achieve effective refilling process for the central keyhole in conventional FSSW joints, a new refilling technique was invented by MUTHUKUMARAN in 2008 [31] known as friction stir spot welding with refilling by friction forming process (FSSW-FFP) instead of complex and expensive refill FSSW machine. This method is dependent on the frictional heat generated by the friction forming process to achieve desired material flow on the surface of an additional plate (filler plate) made of ductile material using a suitable external tool [26,32].

In the present study, it was relied on this new refilling technique to produce friction stir spot welds with refilled keyhole in order to compare them with the other welds manufactured by conventional FSSW process. The mechanical properties (tensile shear load and microhardness) of both conventional FSSW and refill FSSW are evaluated. The microstructure and bonding characteristics are discussed based on the experimental observations. The fracture surface of the failed tensile-shear test specimens was analyzed in detail using the scanning electron microscope.

2. EXPERIMENTAL WORK

AA2024-T3 aluminum alloy with 2mm sheets thickness were chosen as the base material for the present study. The chemical composition is listed in Table 1. In order to find out the mechanical properties and temper condition of the base material, a tensile test was conducted to make sure that material is correspond to the standard requirements of AA2024-T3 according to ASTM. Standard tensile test specimens were cut using CNC wire cut machine in parallel to the rolling direction according to ASTM-E8 [33]. Figure 2 shows the standard dimensions of the tensile test specimen. Table 2 shows the results of mechanical properties for material used in this work.

Table 1: Chemical composition of AA2024 aluminum alloy sheets used in this work (wt %)

Si	Fe	Cu	Mn	Mg	Cr	Ni	Zn	Ti	V	Ga	Al
0.103	0.197	4.84	0.645	1.5	0.027	0.006	0.181	0.042	0.017	0.016	Bal.

Table 2: Mechanical properties of AA2024-T3 aluminum alloy used in this work

Tensile Strength (MPa)	Yield Strength (MPa)	Elongation (%)
486	360	20

International Journal of Engineering Research & Technology (IJERT)
ISSN: 2278-0181
Vol. 6 Issue 04, April-2017

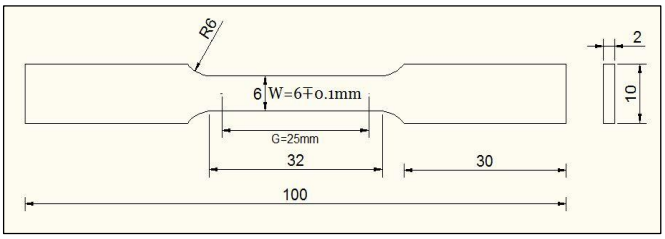

Figure 2: Standard dimensions of the tensile test specimen (All dimension in mm) [33]

According to American Welding Society (AWS) resistance welding handbook [34], the overlap configuration is prepared to produce friction stir spot welded specimens in the dimensions of 175mm, 25mm and 25mm in length, width and overlapping length, respectively, as shown in Figure 3. A vertical milling machine model King XW6032B was used to manufacture all friction stir spot welded samples.

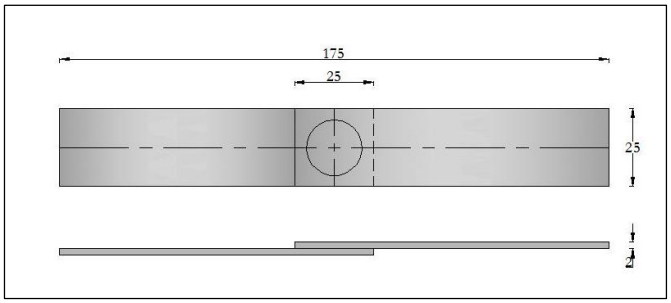

Figure 3: Dimensions of the overlap specimen that to be welded (All dimensions in mm)

The conventional-and refill-FSSW tools was fabricated from tool steel AISI D3 (labeled as X210Cr12) with hardness of 58 HRC. The chemical composition of the tools material is listed in Table 3. In conventional FSSW, two different tools have been used, which have cylindrical and triangular pin profiles, each one of them consists of a flat shoulder with diameter of 18 mm. The diameter of the cylindrical pin and the circle diameter, which is the circumference of the triangular pin, was 5 mm, respectively. It is necessary that the corners of triangular pin were beveled in order to reduce the stress concentration [35]. In refill FSSW, two types of tools, namely conventional tool (C-Tool) and friction forming tool (FFTool), were used in this technique. Conventional tools are similar to the conventional FSSW tools, which also consists of two geometries with the same dimensions and shapes of the tools that used in conventional FSSW process. Friction forming tool is a pinless tool, where consists of a shoulder has an 18 mm diameter with a convex tip profile in a tilt angle of (3º), was used for refilling process. Figure 4 shows the conventional and friction forming tools used in this work.

Table 3: Chemical composition of tool steel X210Cr12 used in this work (wt %)

C	Mn	P	S	Si	Cr	V	Mo
2.11	0.35	0.06	0.02	0.21	12	0.11	0.17

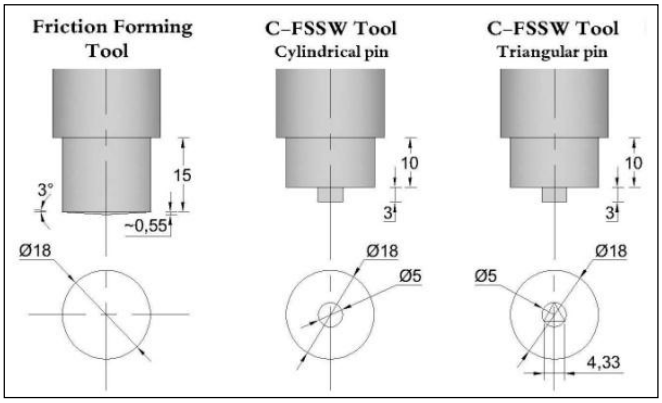

Figure 4: Shapes and dimensions of the conventional-and refill-FSSW tools used in this work (All dimensions in mm)

International Journal of Engineering Research & Technology (IJERT)
ISSN: 2278-0181
Vol. 6 Issue 04, April-2017

Refill friction stir spot welding (RFSSW) process was consisted of two stages: welding and refilling. In the first stage, welding is done in the same three phases of conventional FSSW process. After welding stage, a keyhole is formed in the welded joint due to retraction of the tool, see figure 5(a). In the second stage, namely refilling process, a refill disc of same material and thickness as that of weld sheets is put on the center of upper surface of the keyhole, as shown in Figure 5(b). The non-rotating FFTool is descended downward toward the welded specimen until it touches the refill disc, as shown in Figure 5(c), then rotated at predefined rotational speeds with in a period of time to preheating the refill disc. The rotational speed of friction forming tool must be matched to the tool speed that used in the first stage of refill FSSW process. The refill disc is squeezed slowly downward toward the welded specimen using the rotating FFTool until reaches to a predefined squeezing depth. The rotating tool is left at the specified depth for a period of time, which is named a forming time. In the final step, the rotating FFTool is withdrawn from the workpiece, by a slow rate, leaving behind a friction stir spot welded joint without a keyhole, as shown in Figure 5(d).

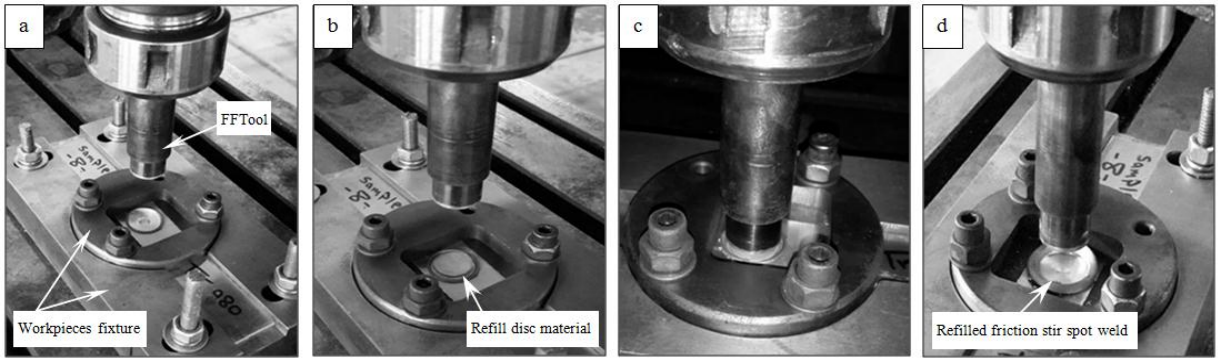

Figure 5: Refill FSSW process, (a) keyhole formed after the welding stage, (b) placing the refill disc on center of the spot welded, (c) touching the non-rotating FFTool on the upper surface of the refill disc, and (d) FSSWed joint with a refilled keyhole

The high pressure and temperature generated by the rotating FFTool leads to occur a high plastic deformation, which results in flowing of filler disc material into the pin hole and forming a metallurgical bonds between the deformed disc material and the surfaces of the keyhole. The other process parameters that related to the welding and refilling stages within refill friction stir spot welding are shown in Table 4.

Table 4: Presents the process parameters used in the first and second stages of the RFSSW

RFSSW Stages	RFSSW Parameters	
1st stage (Welding)	Rotational speeds (rpm)	535, 980, 1325
	Shoulder plunge rate (mm/min)	~0.47
	Shoulder plunge depth (mm)	0.4
	Dwell time (sec)	2
2nd stage (Refilling)	Rotational speeds (rpm)	535, 980, 1325
	Refill disc diameter (mm)	16
	Preheating time (sec)	3
	Forming time (sec)	6
	Squeezing feed rate (mm/min)	~0.65
	Squeezing depth (mm)	2

After welding, macro and microstructure examinations were conducted on the friction stir spot welded specimens. Keller's macroetchant consisting of 50 ml distilled water, 25 ml HNO_3 , 15 ml HCl and 10 ml HF was used to reveal special features of the welding zone. Keller's microetcant consisting of 190 ml distilled water, 5 ml HNO_3 , 3 ml HCl, and 2 ml HF was used to reveal the grain boundaries and other microstructure features of different welding zones.

The Vickers microhardness test was performed on the cross-section of the friction stir spot welded specimens. Microhardness measurements were taken in a horizontal axis along the width of the cross-sectional surface using a diamond pyramid indenter with a load of (500 g.f) and dwell time of (15 sec). In order to evaluate the hardness variation across different regions of the friction stir spot welds, two series of indentations were carried out respectively along two parallel lines at the mid-thickness of upper and lower sheets with a spacing of (0.5mm) between neighboring indents, as shown in Figure 6.

International Journal of Engineering Research & Technology (IJERT)
ISSN: 2278-0181
Vol. 6 Issue 04, April-2017

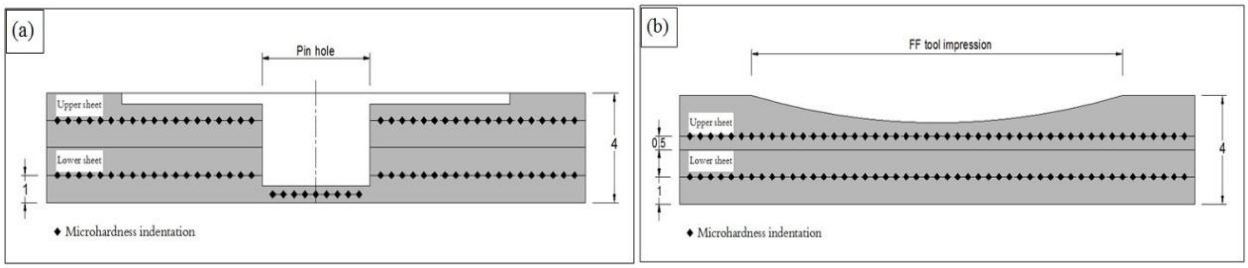

Figure 6: A schematic illustrates distribution of microhardness indentations on the cross section surface, (a) CFSSW specimen, (b) RFSSW specimen (All dimensions in mm)

The tensile-shear test specimens were prepared according to the dimensions shown in Figure 7. They were tested by a computerized universal testing machine at constant cross head speed of (1mm/min). Small pads, which are called shims, have same thickness as welded materials were attached to the test specimen at end of each side in order to minimize rotation of weld nugget during testing and to avoid problem of bending in the grips of the testing machine. The load and displacement were simultaneously recorded during the test. For each welding condition, three specimens were tested and average of three values obtained was taken to evaluate the weld strength.

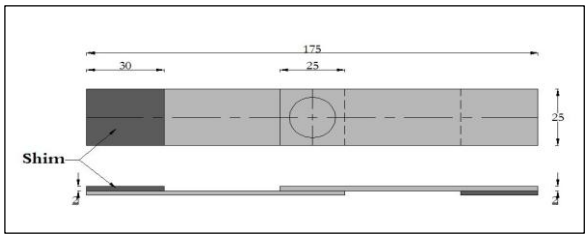

Figure 7: A schematic representation of the lap shear test specimen (All dimensions in mm)

3. RESULTS AND DISCUSSION

3.1 Macro and Microstructure

Figure 8 shows the optical microstructure of the base material of AA2024 aluminum alloy in T3 condition (longitudinal section). The base material consists of elongated grains parallel to the rolling direction and a large number of second-phase particles (Al_2Cu) distributed in matrix. The average grain size of the base material was approximately (35.7µm).

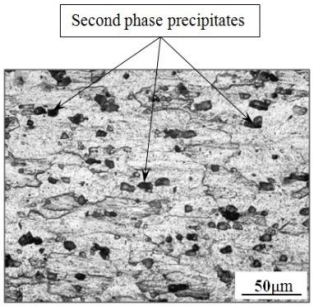

Figure 8: Microstructure of AA2024-T3 base material.

Figure 9 shows the macroscopic appearance of a cross-section of welded specimen made by conventional FSSW process. The cross-section of the friction stir spot welded specimen can be divided into three distinct regions, which are, in sequence, the stir zone (SZ), thermo mechanical affected zone (TMAZ), and the heat affected zone (HAZ) as marked in Figure 9(a_1), (a_2) and (a_3), respectively.

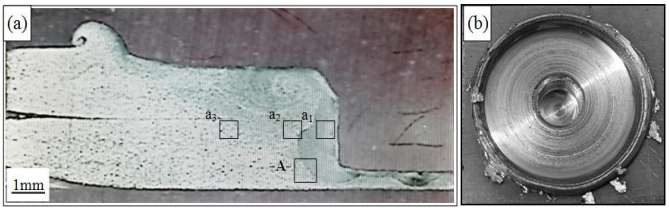

Figure 9: (a) A macroscopic appearance of the cross-section of a conventional FSSW specimen made by the triangular tool pin profile at rotational speed of 535 rpm, (b) a top view of the weld

International Journal of Engineering Research & Technology (IJERT)
ISSN: 2278-0181
Vol. 6 Issue 04, April-2017

The stir zone consists of refined and equiaxed grains due to dynamic recrystallization occurred in periphery of the tool pin, caused by high frictional heating and intense plastic deformation during FSSW process. The precipitates are broken into particles and dissolved in the SZ due to stirring action and high temperature generated by friction, see figure 10(a_1). The TMAZ is characterized by highly deformed and elongated grains. This region is greatly affected by severe plastic deformation of materials occurred in the vicinity of the rotating pin, but the temperature in TMAZ is not sufficient enough to cause recrystallization. The grain size observed in this region is coarser than stir zone (SZ) and finer than heat affected zone (HAZ) as shown in figure 10(a_2). Next to the TMAZ is the HAZ, which consists of undeformed coarse grains, because it has only experienced to the frictional heat. The grain structure in HAZ was not mechanically affected by plastic deformation as shown in Figures 12(a_3). All of these findings are in agreement with previous studies [20, 36, 37, 38, 39].

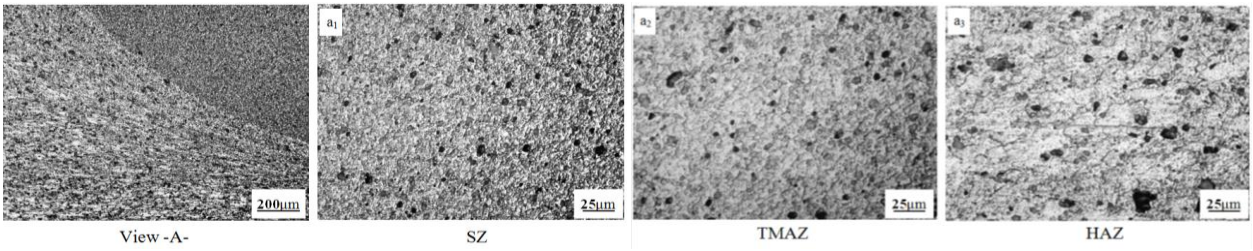

Figure 10: Microstructures of the cross-section of a conventional FSSW specimen, (view-A-) close-up view of region A marked in Figure 9(a), and (a_1, a_2, a_3) close-up views of regions a_1 – a_3 marked in Figure 9(a), respectively

Figure 11 shows the macroscopic appearance of a cross-section of welded specimen made by refill FSSW. It is clear that the keyhole was successfully refilled by the RFSSW process. In addition, weld defects such as incomplete refilling, lack of mixing, no mixing, and voids are completely eliminated in this study. This is the originality of the present study, and what distinguishes this work among other works and researches is the possibility of obtaining a defect-free joint made by friction stir spot welding process without presence of the central hole. As shown from figure 11(b), there is an impression on the top surface of the refilled spot weld with a profile matches the convexity of the friction forming tool.

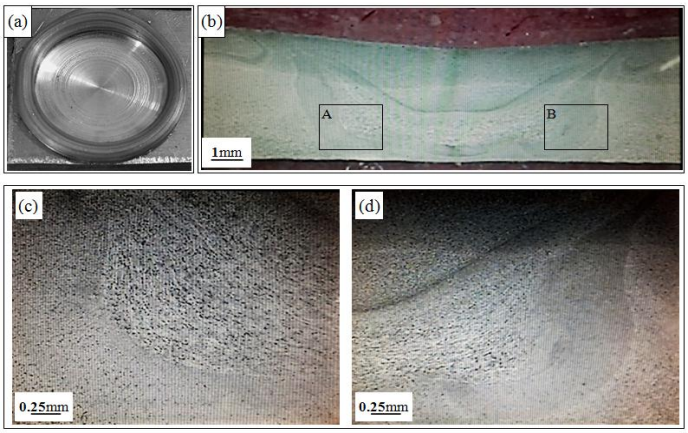

Figure 11: Macrostructures of a cross-section of refill FSSW specimen, (a) a top view of the weld, (b) a cross-sectional view, and (c, d) close-up views of regions A and B marked in (b), respectively.

Figures (12 and 13) show the macroscopic appearance and microstructures, respectively, of a welded joint made by refill FSSW. From figure 13, the close-up views of micrographs (a) and (b) represents the SZ, and TMAZ, respectively, marked by (a – b) shown in Figure 12. It is revealed that the division of weld regions in refill FSSW specimen is similar to that welded by conventional FSSW.

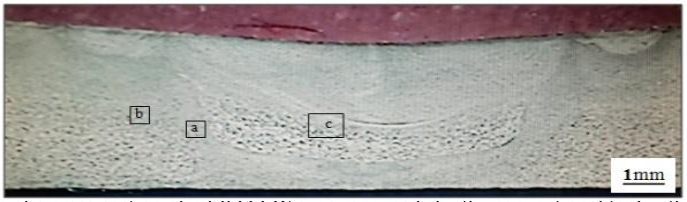

Figure 12: Macroscopic appearance of a cross-section of refill FSSW specimen made by the conventional tool with a cylindrical pin at rotational speed of 535 rpm.

International Journal of Engineering Research & Technology (IJERT)
ISSN: 2278-0181
Vol. 6 Issue 04, April-2017

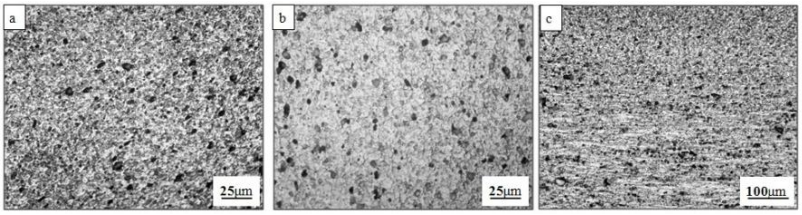

Figure 13: Microstructures of a cross-section of refill FSSW specimen welded by the conventional tool with a cylindrical pin at rotational speed of 535 rpm, (a, b, and c) close-up views of refill FSSW regions (a – c) marked in Figure 12

In the refilled zone (RZ), average of grain size is increased from the top to bottom, see Figure 13(c). As shown from figure 14, the RZ is consists of a very fine grains (13.4μm) at the top, while at the bottom, the microstructure is characterized by a coarse grains (39.47μm). This is may be attributed to the high frictional heat and severe plastic deformation in the region beneath the tip of FFTool during the refilling process [32, 40]. Therefore, the refilled material at the top has the strongest tendency to dynamic recrystallization, and subsequently, the microstructure is greatly refined. While the material at the bottom is undergoing to partial plastic deformation because of the frictional heat in this region is not sufficient to occurrence dynamic recrystallization. In addition to the shorter thermal cycle at the bottom compared with the top, this is may be because of the deformed material at the bottom is in contact with unaffected surfaces of the pin hole, as well as the workpiece that to be refilled is in contact with the workpieces fixture. So, the refilled material at the bottom is characterized by a coarse grain structure.

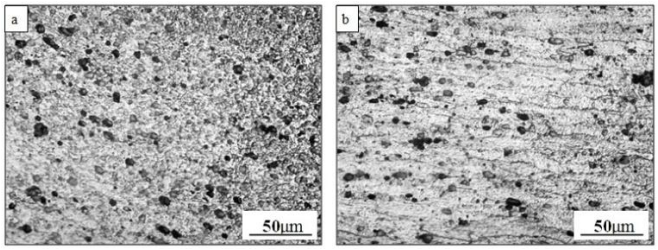

Figure 14: Microstructure of the RZ in a refill FSSW specimen, (a) transition between the top and middle regions within the RZ, (b) the bottom of the RZ

The bonding conditions between two sheets in overlap configuration can be categorized in three main regions exist in sequence from periphery of the tool-pin hole towards the end of the welded sheets, which are completely bonded region, partially bonded region (Kissing bond), and unbonded region [37], as shown in Figure 15(a). The extension of these three regions is called as Hook, which is a characteristic feature of the friction stir spot welded joints.

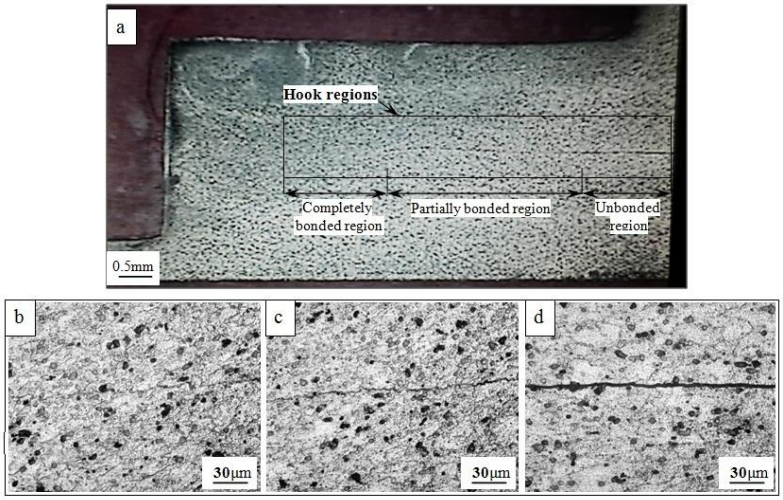

Figure 15: Typical cross-sectional views show the bonding regions in conventional FSSW specimens welded by different tool pin profiles, (a) a cross-sectional macrograph, (b,c, and d) close-up views of completely bonded region, partially bonded region, and unbonded region, respectively

It is evident from Figure 15 that the hook has a straight shape, and its regions directed perpendicular to the keyhole. In completely bonded region, interface of the welded sheets surfaces cannot be identified and the grains

International Journal of Engineering Research & Technology (IJERT)
ISSN: 2278-0181
Vol. 6 Issue 04, April-2017

from both sheets are completely mixed, see figure 15(b), that is due to severe plastic deformation and stirring action occurred in this region. Next to completely bonded region is a partial bonded region, where non uniform mixing is observed due to insufficient stirring and frictional heating, see figure 15(c). However, joint interface below tool shoulder is found to be mechanically bonded due to effect of shoulder squeezing only. In the last region (unbonded), there is no stirring occurred at the interface of the two sheets because it is away from the rotating tool pin and is near at the end of sheets, see figure 15(d) [37]. The plastic flow of upper and lower sheets materials during FSSW process leads to hook formation [38].

Figure 16 shows the microstructure of the SZ in RFSSW specimens welded by the rotational speed of 535 rpm using the conventional tools with cylindrical and triangular pin profiles, respectively. It is evidence from these figures there is a clearly difference in the grain size of the spot welds between the specimens fabricated by different pin profiles under the same process conditions. For the purpose of comparison between these figures, the triangular pin resulted in a stir zone with finer grain structure than the cylindrical tool pin profile. Based on figure 16(a, and b), the average grain size in the SZ of refill FSSW specimen welded by the cylindrical pin is (10.86μm), while in the welded specimen made by the triangular pin is (9.62μm). This is indicates that the triangular pin causes more severe plastic deformation in welding material than the cylindrical pin, because of the triangular pin caused flowing of the plasticized material back and forth in the radial direction over a wider region during the welding stage. In contrast, cylindrical pin caused flowing of material only around its own axis [41, 42, 43].

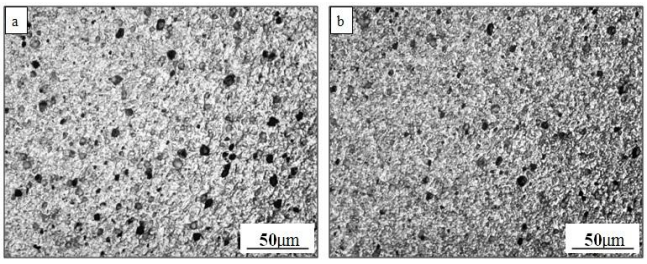

Figure 16: Microstructure of the SZ in refill FSSW specimens welded by the conventional tools with different pin profiles at rotational speed of 535 rpm, (a) Cylindrical pin, (b) Triangular pin

Figures (17 – 19) show the microstructure of the RZ in refill FSSW specimens welded by the conventional tools with different pin profiles at the rotational speeds of (535, 980 and 1325) rpm, respectively. From these figures, it can be seen that the grain structure of the RZ becomes coarse with increasing tool rotational speed, as clearly shown in Figure 17(a,c) and Figure 19(a,c). This is may be attributed to the excessive heat input caused by rotating of the friction forming tool in higher rotational speeds during the refilling process, led to coarsening of the grains, as shown in figures 17(c) and 19(c) [44].

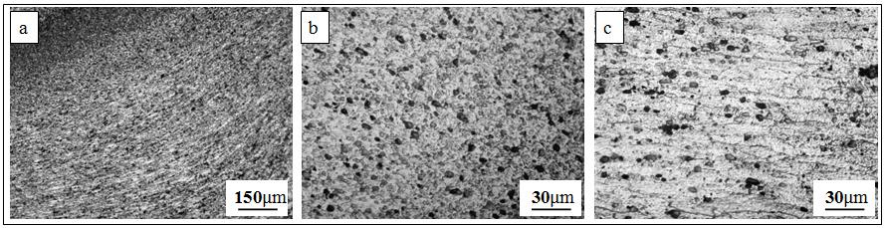

Figure 17: Microstructure of the RZ in the refill FSSW specimen welded by the conventional tool with a triangular pin at rotational speed of 535 rpm; (a) Overview of the RZ, and (b, and c) close-up views of the top and bottom of the RZ, respectively.

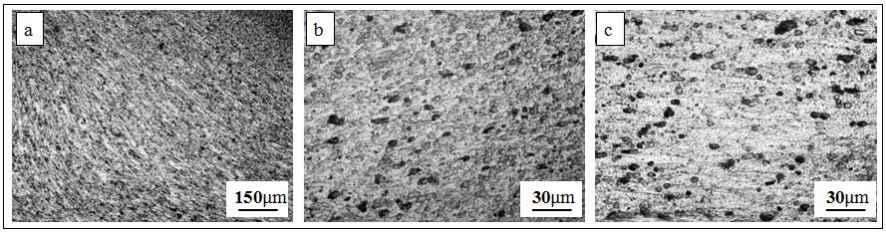

Figure 18: Microstructure of the RZ in the refill FSSW specimen made by the conventional tool with a triangular pin at rotational speed of 980 rpm; (a) Overview of the RZ, and (b, and c) close-up views of the top and bottom of the RZ, respectively.

International Journal of Engineering Research & Technology (IJERT)
ISSN: 2278-0181
Vol. 6 Issue 04, April-2017

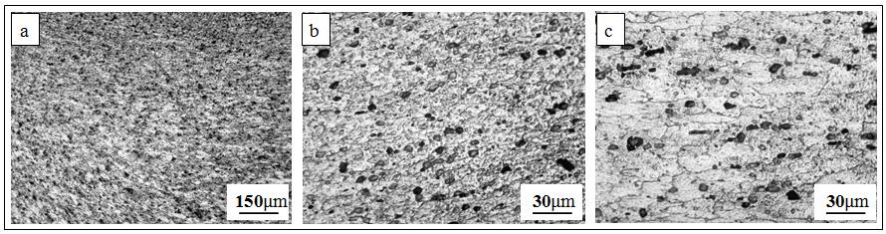

Figure 19: Microstructure of the RZ in the refill FSSW specimen made by the conventional tool with a cylindrical pin at rotational speed of 1325 rpm; (a) Overview of the RZ, and (b, and c) close-up views of the top and bottom of the RZ, respectively.

3.2 Microhardness

Figures (20 and 21) show the influence of refilling process on microhardness values on along the cross-section of welded specimens made by the conventional tools with cylindrical and triangular pin profiles, respectively, at the rotational speed of 535 rpm. According to the microhardness profiles illustrated in these figures, distribution of Vickers hardness is found to be nearly symmetric with respect to the center of the spot, furthermore, the welds showed higher microhardness in periphery of the keyhole, specifically in the SZ, and gradually decreases through TMAZ and reaches the minimum value in the HAZ, then increases towards the base material. The reduction in Vickers hardness in the HAZ can be attributed to the coarsening of grains and growth of strengthening precipitates due to overaging caused by the effect of thermal cycle during FSSW processes, which resulted in the lower hardness than that of the base material according to the Hall-petch relationship [29,40], as follows the equation:

$$HV = H_o + K_H d^{-½} \quad \text{..... equation (1) [40]}$$

Where (d) is the grain size, (H_o) and (K_H) are material constants. According to the above equation, when the average grain size increases, the hardness decreases. While in the SZ and TMAZ, the grains subjected to severe plastic deformation besides high frictional heat, as previously mentioned in section (3.1), which led to appearance of fine grain structure in these regions, see figure 10, particularly the SZ undergo dynamic recrystallization due to the higher temperature during friction stir spot welding. Thus, Vickers hardness increased in the SZ due to the finer microstructure than that existence in the base material.

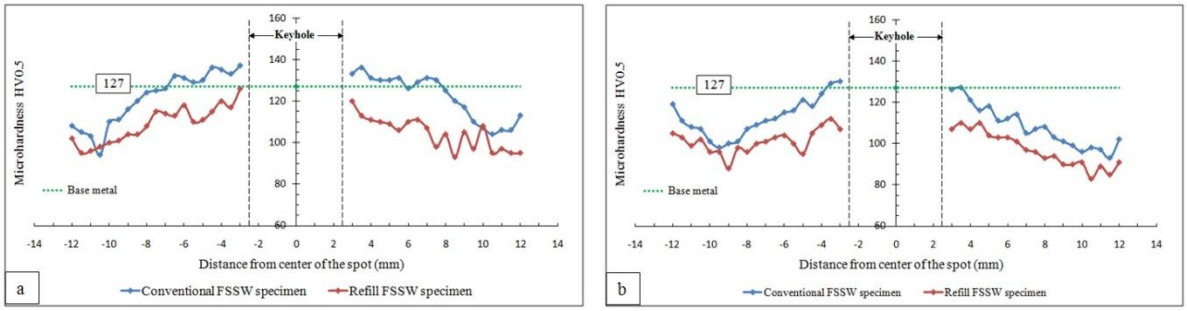

Figure 20: Microhardness profile on along the cross-section of welded specimens made by CFSSW and RFSSW at the rotational speed of 535 rpm using the cylindrical tool pin profile, (a) upper sheet, (b) lower sheet.

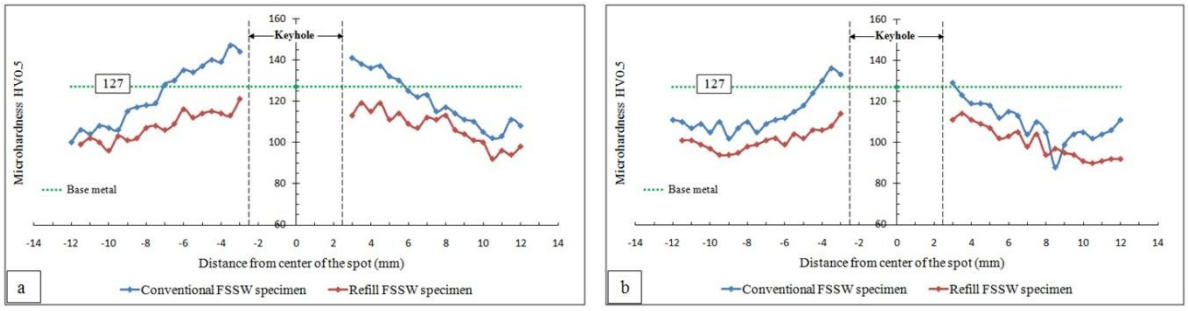

Figure 21: Microhardness profile on along the cross-section of welded specimens made by CFSSW and RFSSW at the rotational speed of 535 rpm using the triangular tool pin profile, (a) upper sheet, (b) lower sheet.

International Journal of Engineering Research & Technology (IJERT)
ISSN: 2278-0181
Vol. 6 Issue 04, April-2017

It is clear from the above figures that the microhardness profile on along the upper and lower sheets of refill FSSW specimens has similar characteristics to that of conventional FSSW samples. In refill FSSW specimens, the Vickers hardness reached the minimum in HAZ, and increased gradually in TMAZ and SZ toward the center of the spot. But, it can be seen that microhardness values in all welding zones decreased, compared with the average microhardness of base material (127 HV0.5), after refilling Figure 22, shows the effect of increasing the rotational speeds of friction forming tool on microhardness profile along the top and bottom of the refill zone in the spot welds made by refill FSSW process. As shown from this figure in both of the top and bottom of the RZ, Vickers hardness value at the center of weld increased with increasing in tool rotational speed during the refilling process. Also, it can be seen that the microhardness profile at the rotational speed of 535rpm is the lowest compared with the average hardness of the base material as well as that of the RZ welded at the higher rotational speeds (980, and 1325) rpm. While the highest hardness value at the most measurements is observed at the tool rotational speed of 1325rpm.

process. This is may be because of the higher heat input caused by the refilling process, which caused dissolution of fine precipitates in the regions that were exposed to severe plastic flow, especially in the SZ, and also caused softening in the other regions that were subjected to the effect of thermal cycle due to coarsening of precipitates and grains [40]. Such a microstructure change causes a reduction in microhardness values in the refill FSSW specimens.

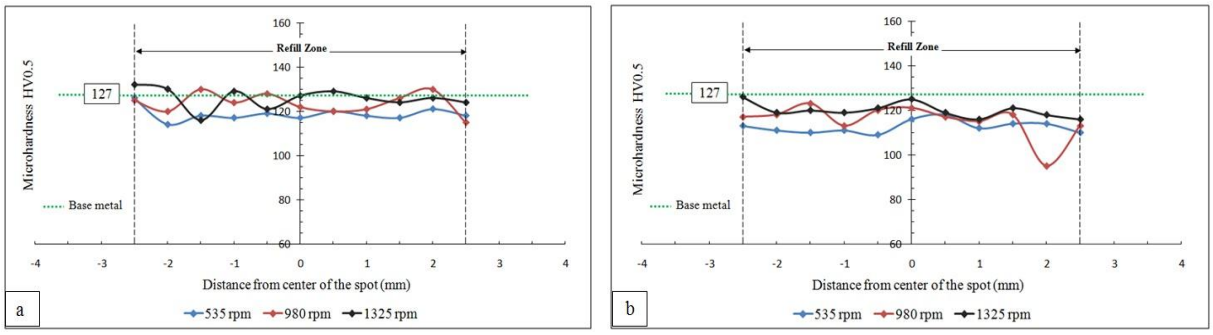

Figure 22: Microhardness profile on along the top and bottom of the RZ in welded specimens made by the refill FSSW at different rotational speeds; (a) the top region, (b) the bottom region.

It is clear from the results plotted in the above figures that microhardness in the refill zone increased with increasing the tool rotational speeds. This indicates that the dominant factors governing the hardness in RZ are the size and distribution of strengthening precipitates more than the variations in grain size [45, 46, 47], see figure 14. F. GEMME et al [48], when studying the effect of welding parameters on mechanical properties of friction stir welded joints of aluminum alloy sheets, stated that the precipitation state plays a crucial role on microhardness of AA7075-T6 welds and other heat-treatable aluminum alloys because of AA7075 in T6 condition contains a large number of submicroscopic Al_2CuMg precipitates, which render a high hardness in this alloy. Hence, it can be concluded that increase in microhardness of the refill zone is may be due to the comprehensive effect of the higher frictional heat and more severe plastic flow resulted from the higher tool rotational speed during the refilling process, which caused increasing in the dynamic recrystallization rate led to formation of finer precipitates in the RZ, especially at the top region. Therefore, microhardness of the RZ increased at the highest tool rotational speed.

3.3 Tensile Shear Strength

A comparison between CFSSW and RFSSW in terms the effects of tool rotational speeds and tool pin geometry on the weld strength is shown in Figure 23.

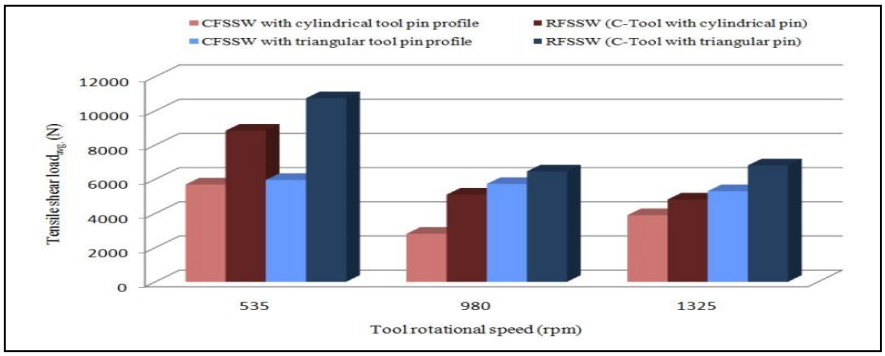

Figure 23: Tensile shear load of the spot weld in all FSSW joints made by conventional FSSW and refill FSSW processes at different tool rotational speeds and tool pin profiles.

International Journal of Engineering Research & Technology (IJERT)
ISSN: 2278-0181
Vol. 6 Issue 04, April-2017

From the general comparison of the tensile-shear test results shown in Figure 23, it is clear that 535 rpm was the dominant rotation speed which gave the higher weld strength in all FSSW specimens. Also, it can be seen that the weld strength was improved in all conventional FSSW joints after refilling the pin hole, especially in the conventional FSSW joints made by the cylindrical pin at the tool rotational speed of 980 rpm, the lowest tensile-shear load was increased from (2807 N) to (5097 N) after refilling process. For the purpose of evaluating the improvement in welding strength after conducting the refilling process, see Table 5.

Table 5: Improvement of weld strength in the FSSW joints after conducting refilling process

No.	Tool Pin Profile	Rotational Speed (rpm)	Conv. FSSW Specimens	Refill FSSW Specimens	Improvement in Tensile-Shear Load (%)
			Tensile-Shear Load $_{avg.}$ (N)	Tensile-Shear Load $_{avg.}$ (N)	
1	Cylindrical	535	5690	8839	35.6
2	Cylindrical	980	2807	5097	45
3	Cylindrical	1325	3896	4812	19
4	Triangular	535	5956	10737	44.5
5	Triangular	980	5722	6456	11.3
6	Triangular	1325	5302	6808	22

The improvement in welding strength is attributed to the absence of the pin hole in FSSW joints. This is because of the presence of the pin hole in conventional FSSW joints acts as notch during tensile loading and causes stress concentration leads to initiation and propagation of cracks through the weld nugget [37, 49]. Also, the presence of extra material in the weld area, due to the refill disc addition, resulted in an increase of effective cross-sectional area of weld nugget, which causes the improvement in tensile-shear load of the refill FSSW joints [32].

Four different failure modes were observed in the failed specimens under tensile shear loading: (shear, tensile-shear mixed, nugget pullout and plug-type on the upper sheet) failure modes. Figure 24 shows close-up top views of the lower sheets and close-up bottom views of the upper sheets of conventional FSSW and refill FSSW joints under tensile-shear tests.

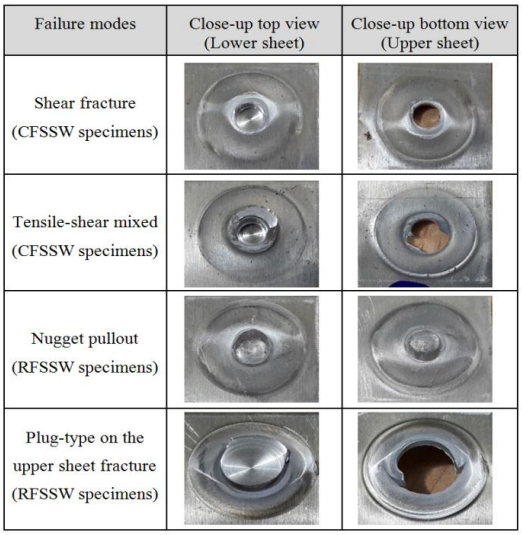

Figure 24: Close-up views of different modes of fracture under tensile-shear tests.

Shear failure occurred in the specimens which have low tensile shear strength. It was observed in conventional FSSW specimens welded by the cylindrical tool-pin profile at all rotational speeds used in this study. The fracture is propagated in horizontal direction along the boundary between the welded sheets due to tensile loading. The final fracture is occurred only through the stir zone because the tool pin indentation can be recognized without any damage.

Tensile-shear mixed failure mode is observed in conventional FSSW specimens welded by the triangular tool pin profile at all rotational speeds. In this mode, the fracture partly occurred in the stir zone in one side of the spot weld and partly in the upper sheet in the opposite side.

The nugget pullout failure mode was noticed in refill FSSW specimens welded by the conventional tool with a cylindrical pin profile at all rotational speeds. As shown from figure 24, some of the weld nugget is remained on the

International Journal of Engineering Research & Technology (IJERT)
ISSN: 2278-0181
Vol. 6 Issue 04, April-2017

lower sheet, while, most of the nugget pulled out with the upper sheet. This indicates that best mechanical bonding was achieved between the refill disc material and the pin-hole surfaces due to the refilling process.

Plug-type on the upper sheet failure mode was observed in refill FSSW specimens made by the conventional tool with a triangular pin profile at all rotational speeds. The weld nugget is completely withdrawn from the upper sheet and remained in the lower sheet leaving a circular hole in the refilled zone of the upper sheet. This suggests that the failure started at the periphery of the refilled hole and propagated across thickness of the upper sheet. In this work, FSSW specimens which are failed in a plug-type failure mode showed higher weld strength than those failed with the other modes.

3.4 SEM Examination

Scanning Electron Microscope (SEM) was used to characterize the fracture surfaces of refill FSSW specimens after tensile-shear testing. Fracture surface of the base material (AA2024-T3 aluminum alloy sheet), as observed under SEM, is shown in Figure 25. Fine equiaxed dimples and hemispherical microvoids are observed on the fractured surface, indicating ductile failure of the base material under tensile shear loading.

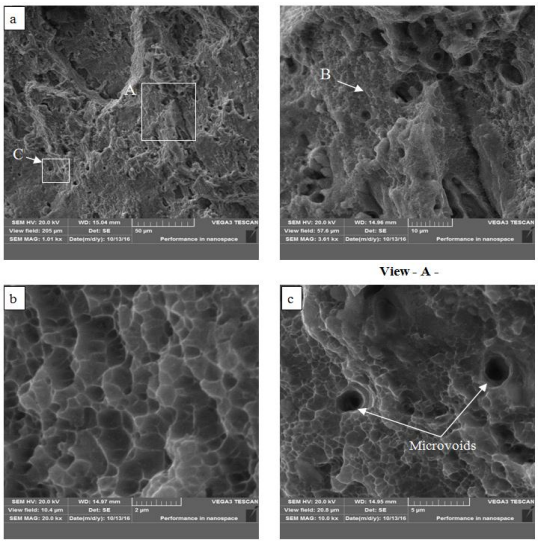

Figure 25: Scanning electron micrographs of base material AA2024-T3 aluminum alloy sheet after tensile testing, (a) Overview of fractured surface, (b) Magnified view of region B marked in view -A- , (c) Magnified view of region C marked in (a) showing equiaxed dimples and micro voids

Figures (26 and 27) show SEM images of fractured surface observed in the lower and upper sheets, respectively, of a refill FSSW specimen failed in nugget pullout-type failure mode. The ridge-type (weld nugget) in regions A and B, marked in figure 26(a), was pulled out due to the effect of tensile shear loading. Different appearances of dimples were noticed in fracture surfaces of regions A, B, and C. Fracture surface with striation-like pattern containing few small shallow dimples was observed at region A, see figures 26 (view-A-) and (b), while a fracture surface with more dimples was seen at region B. These dimples are bigger and dipper than those in region A, as shown in figure 26(c). This indicates that the crack was initiated at the parent sheets interface and propagated circumferentially a cross the stir zone at region A, and then directed in a circumferential direction along weld nugget through region B. The final fracture has occurred at region C as indicated from the presence of more equiaxed dimples elongated in direction of tensile-shear force as shown in Figure 26(d).

In the center of failed nugget, fracture surface of the regions D and E, marked in figure 26(a), exhibit very small elongated dimples as shown in figure 26(e). This indicates the existence of a well bonding between the refill disc material and the bottom surface of the pin hole caused by the refilling process. Also, it can be seen that some parts of the pulled nugget remained welded at the center of fracture surface in the lower sheet after failure, see figure 26(f).

International Journal of Engineering Research & Technology (IJERT)
ISSN: 2278-0181
Vol. 6 Issue 04, April-2017

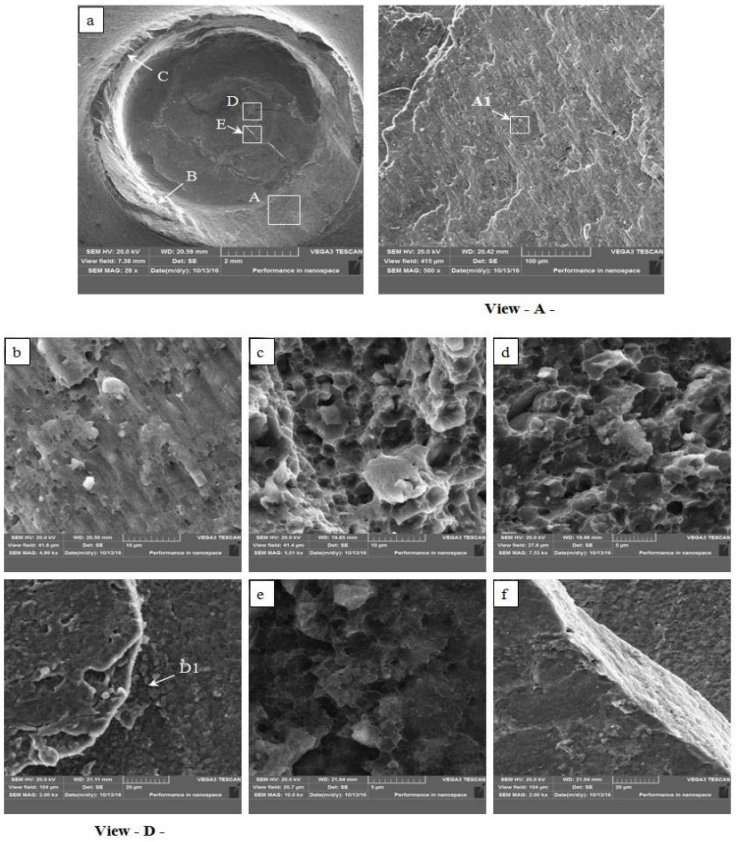

Figure 26: SEM images of refill FSSW specimen failed in nugget pullout-type failure mode, (a) Overview of failed nugget in the lower sheet, (b) Magnified view of region A1 marked in (view-A-), (c, d) Magnified views of regions B and C marked in (a), respectively, (e) Magnified view of region D1 marked in (view-D-), (f) Magnified view of region E marked in (a)

Most of the failed nugget has pulled out with the upper sheet as shown in figure 27(a). Figure 27 (b - e) show the fracture surfaces of failed nugget in the upper sheet at different regions (A - D). Fracture surface in regions A and B corresponds with surface morphology of regions A and C, respectively, that were observed in failed nugget of the lower sheet, see figure 26(b, d), which indicates that the failure has occurred in the same direction a cross weld nugget. As shown from the SEM micrographs of regions A and B, there are exist numerous of small shallow dimples in region A, see figure 27(b), indicating the crack initiation at this region, while at region B, there are exist more elongated dimples, see figure 27(c), which indicates that a fracture surface at the final stage of failure. The existence of some parts of the lower failed nugget welded at nugget of the upper sheet, see figure 27(d), in addition to the presence of elongated dimples observed in magnified view of region D, as shown in figure 27(e), gives a prove that the metallurgical bonding was formed between the deformed disc material and the bottom surface of the pin hole due to severe plastic flow caused by the refilling process.

International Journal of Engineering Research & Technology (IJERT)
ISSN: 2278-0181
Vol. 6 Issue 04, April-2017

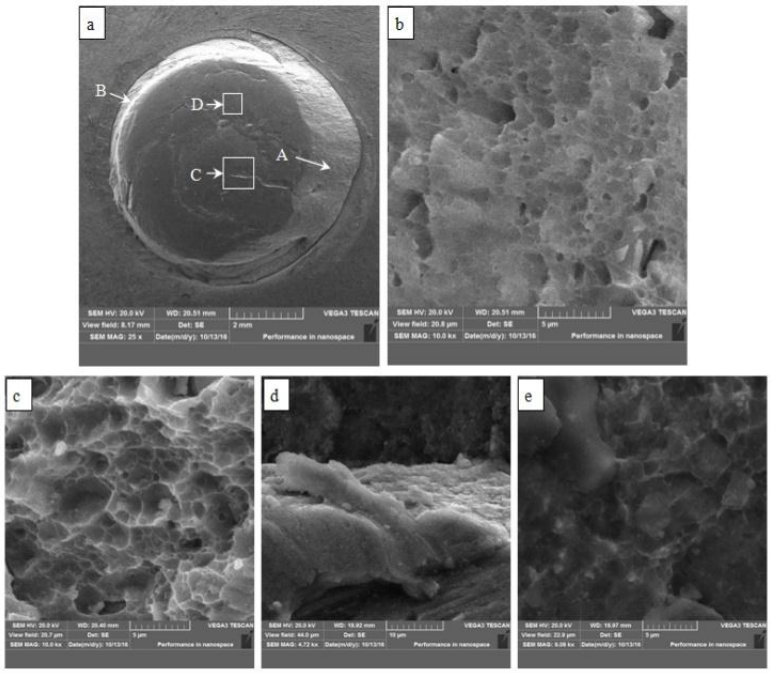

Figure 27: SEM images of a refill FSSW specimen failed in nugget pullout-type failure mode, (a) Overview of failed nugget in the upper sheet, (b, c, d, and e) Magnified views of regions A, B, C, and D marked in (a), respectively.

Figure 28, shows SEM micrographs of fracture surface of a refill FSSW specimen failed in plug-type failure mode. Based on these micrographs, it is believed that the crack initiated at periphery of weld nugget and propagated circumferentially upward in a vertical direction across the upper sheet thickness through region B marked in figure 28(view-A-). This is because of the SZ resisted the crack propagation in a horizontal direction [36]. Finally, fracture has occurred in region C at the final stage of failure, as shown in figure 28(c). Also, it can be observed that whole failed nugget remained welded in the lower sheet after failure, and the final fracture has occurred circumferentially across friction forming indentation at the upper sheet, which indicates that the conventional tool with a triangular pin resulted in a spot weld with harder and stronger stir zone than that produced by the conventional tool with a cylindrical pin profile during RFSSW.

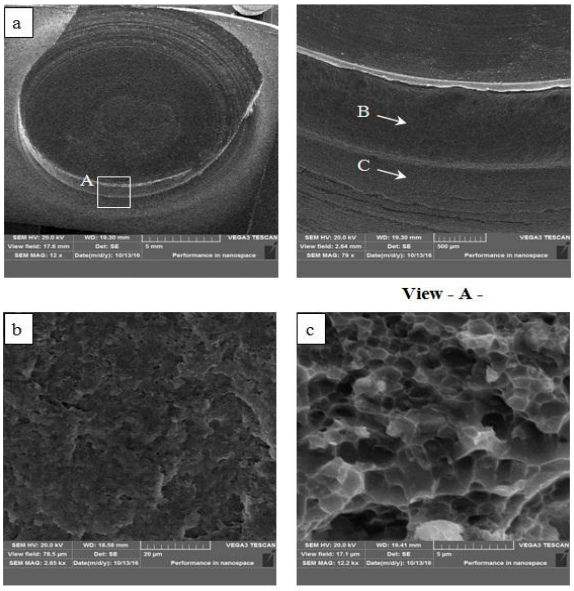

Figure 28: SEM fractographs of a refill FSSW specimen failed in plug-type on the upper sheet failure mode, (a) Overview of failed nugget on the lower sheet, (b, c) Magnified views of regions B and C marked in (view-A-), respectively

International Journal of Engineering Research & Technology (IJERT)
ISSN: 2278-0181
Vol. 6 Issue 04, April-2017

4. CONCLUSIONS

From the experimental results obtained, one can conclude that the new refill friction stir spot welding (RFSSW) process can be used successfully to produce FSSW joints of AA2024-T3 aluminum alloy sheets without a keyhole. Conclusions from this work are listed as follows:

1. The lowest tool rotational speed (535 rpm) and the triangular tool-pin profile are the optimum welding parameters which gave the higher fracture loads in all FSSW specimens.
2. The maximum tensile shear loads obtained in the refill FSSW and conventional FSSW using the triangular tool pin profile at the same tool rotational speed 535 rpm are (10737 N) and (5956 N), respectively.
3. The improvement of weld strength in the refill FSSW joints can be attributed to the absence of the keyhole and also due to the presence of extra material in the weld nugget.
4. Two distinct failure modes observed in the failed specimens of conventional FSSW under tensile shear loading: shear and tensile-shear mixed failure modes. While other different types of fracture modes, namely nugget pullout and plug-type on the upper sheet failure, were observed in the refill FSSW joints.
5. The tool pin geometry has the stronger effect in determining failure mode of conventional-and refill-FSSW than the effect of tool rotational speeds.
6.

REFERENCES

[1] A. A. M. da Silva, E. Aldanondo, P. Alvarez, E. Arruti and A. Echeverrı´a, "Friction stir spot welding of AA1050 Al alloy and hot stamped boron steel (22MnB5)", Science and Technology of Welding and Joining, Vol.15, No. 8, pp. 682, 2010.

[2] A. Ambroziak and M. Korzeniowski, "Using Resistance Spot Welding For Joining Aluminum Elements in Automotive Industry", Archives of Civil and Mechanical Engineering, Vol. X, No.1, pp. 5-13, 2010.

[3] R.S. Mishra and Z.Y. Ma, "Friction Stir Welding and Processing", Materials Science and Engineering R, Vol. 50, pp. 1-78, August 2005.

[4] D. A. Wang and S. C. Lee, "Microstructures and failure mechanisms of friction stir spot welds of aluminum 6061-T6 sheets", Journal of Materials Processing Technology, Vol. 186, pp. 291-297, 2007.

[5] M. Besharati-Givi and P. Asadi, "ADVANCES IN FRICTION-STIR WELDING AND PROCESSING", 1st edition. [S.l]: WOODHEAD, 2017.

[6] S. Pawar and M. Shete, "OPTIMIZATION OF FRICTION STIR WELDING PROCESS PARAMETER USING TAGUCHI METHOD AND RESPONSE SURFACE METHODOLOGY: A REVIEW", International Journal of Research in Engineering and Technology, Vol. 2, No. 12, pp. 551-554, December 2013.

[7] H. Patil and S. Soman, "Experimental study on the effect of welding speed and tool pin profiles on AA6082-O aluminum friction stir welded butt joints", International Journal of Engineering, Science and Technology, Vol. 2, No. 5, pp. 268-275, 2010.

[8] S. Khodir and T. Shibayanagi, "Microstructure and Mechanical Properties of Friction Stir Welded Dissimilar Aluminum Joints of AA2024-T3 and AA7075-T6", Materials Transactions, Vol. 48, No. 7, pp. 1928-1937, 2007.

[9] P. Prasanna, C. Penchalayya and D. A. Rao, "Optimization and Validation of Process Parameters in Friction Stir Welding on AA 6061 Aluminum Alloy Using Gray Relational Analysis", International Journal of Engineering Research and Applications (IJERA), Vol. 3, No. 1, pp. 1471-1481, January-February 2013.

[10] A. Gupta and S. Patel, "Experimental Evaluation on the Effect of Welding Speed and Tool Pin Profiles on Friction Stir Welded Joints on AA 6082-T6", International Journal of Engineering Research & Technology (IJERT), Vol. 3, No. 5, pp. 2257-2262, May 2014.

[11] T. Iwashita, "METHOD AND APPARATUS FOR JOINING", U.S. Patent 6,601,751 B2, August 2003.

[12] Mazda media release, "Mazda Develops World's First Steel and Aluminum Joining Technology Using Friction Heat", Products and Technology, 2005. [Online], Available: http://www.mazda.com/en/publicity/release/2005/200506/050602.html.

[13] J. Piccini and H. G. Svoboda, "Effect of pin length on Friction Stir Spot Welding (FSSW) of dissimilar Aluminum-Steel joints", Procedia Materials Science, Vol. 9, pp. 504-513, 2015.

[14] EAA: Aluminum Automotive Manual Joining – 7.Solid state welding, 2015. Available at: http://www.alueurope.eu/

[15] W. Yuan, "Friction stir spot welding of aluminum alloys", Masters Theses, Missouri University of Science and Technology, 2008. Available at: http://scholarsmine.mst.edu/masters_theses/5429.

[16] Y. Bozkurt and M. Bilici, "Taguchi Optimization of Process Parameters in Friction Stir Spot Welding of AA5754 and AA2024 Alloys", Advanced Materials Research, Vol. 1016, pp. 161-166, 2014.

[17] A. Reilly, "Modeling of Friction Stir Spot Welding", Ph.D. Thesis, Department of Engineering, University of Cambridge, May 2013.

[18] M. Bilici, "Effect of Tool Geometry on Friction Stir Spot Welding of Polypropylene Sheets", Express Polymer Letters, Vol. 6, No. 10, pp. 805-813, 2012.

[19] Y. Sun, H. Fujii, N. Takaki and Y. Okitsu, "Microstructure and mechanical properties of mild steel joints prepared by a flat friction stir spot welding technique", Materials & Design, Vol. 37, pp. 384-392, 2012.

[20] Y. Uematsu, K. Tokaji, Y. Tozaki, T. Kurita and S. Murata, "Effect of re-filling probe hole on tensile failure and fatigue behaviour of friction stir spot welded joints in Al–Mg–Si alloy", International Journal of Fatigue, Vol. 30, pp. 1956-1966, 2008.

[21] Y. Chen, J. Chen, B. Amirkhiz, M. Worswick and A. Gerlich, "Microstructures and properties of Mg alloy/DP600 steel dissimilar refill friction stir spot welds", Science and Technology of Welding and Joining, Vol. 20, No. 6, pp. 494-501, 2015.

[22] D. Bakavos, Y. Chen, L. Babout and P. Prangnell, "Material Interactions in a Novel Pinless Tool Approach to Friction Stir Spot Welding Thin Aluminum Sheet", Metallurgical and Materials Transactions A, Vol. 42, No. 5, pp. 1266-1282, 2010.

[23] P. Prangnell and D. Bakavos, "Novel Approaches to Friction Spot Welding Thin Aluminum Automotive Sheet", Materials Science Forum, Vol. 638-642, pp. 1237-1242, 2010.

[24] C. Schilling and J. Santos, "METHOD AND DEVICES FOR JOINING AT LEAST TWO ADJOINING WORK PIECES BY FRICTION WELDING", U.S. Patent 6,722,556 B2, April 2004.

International Journal of Engineering Research & Technology (IJERT)
ISSN: 2278-0181
Vol. 6 Issue 04, April-2017

[25] L. Campanelli, U. Suhuddin, J. Santos and N. Alcântara, "Parameters optimization for friction spot welding of AZ31 magnesium alloy by Taguchi method", Soldagem & Inspeção, Vol. 17, No. 1, pp. 26-31, 2012.
[26] Y. Rao, V. Kalyanavalli, D. Sastikumar, S. Muthukumaran and S.Venukumar, "Non-Destructive Evaluation of Aluminum A6061-T6 Welds Produced by Friction Stir spot Welding", National Institute of Technology, Tiruchirappalli, India.
[27] S. Venukumar, S. Yalagi, S. Muthukumaran and S. Kailas, "Static shear strength and fatigue life of refill friction stir spot welded AA 6061-T6 sheets", Science and Technology of Welding and Joining, Vol. 19, No. 3, pp. 214-223, 2014.
[28] M. Tier, T. Rosendo, J. Santos, N. Huber, J. Mazzaferro, C. Mazzaferro and T. Strohaecker, "The influence of refill FSSW parameters on the microstructure and shear strength of 5042 aluminum welds", Journal of Materials Processing Technology, Vol. 213, No. 6, pp. 997-1005, 2013.
[29] Z. Shen, X. Yang, Z. Zhang, L. Cui and T. Li, "Microstructure and failure mechanisms of refill friction stir spot welded 7075-T6 aluminum alloy joints", Materials and Design, Vol. 44, pp. 476–486, 2013.
[30] B. Parra, V. Saccon, N. Alcântara, T. Rosendo and J. Santos, "An investigation on friction spot welding in AA6181-T4 alloy", Tecnologia em Metalurgia Materiais, Vol. 8, No. 3, pp. 184-190, 2011.
[31] S. MUTHUKUMARAN, "An improved friction forming process and a friction forming machine with a tool and fixture", Indian Patent 242420, Application no.137/KOL/2006, August 2010
[32] S. Prakash and S. Muthukumaran, "Refilling Probe Hole of Friction Spot Joints by Friction Forming", Materials and Manufacturing Processes, Vol. 26, No. 12, pp. 1539-1545, 2011.
[33] ASTM E8M, Standard Test Methods for Tension Testing of Metallic Materials, 2004.
[34] American Welding Society ,"Resistance Welding Theory and Use", Reinhold Publishing Corporation New York, Chapman & Hall, LTD ,1956.
[35] M. Paidar, F. Sadeghi, H. Najafi and A. Khodabandeh, "Effect of Pin and Shoulder Geometry on Stir Zone and Mechanical Properties of Friction Stir Spot-Welded Aluminum Alloy 2024-T3 Sheets", Journal of Engineering Materials and Technology, Vol. 137, pp. 031004-1 – 031004-6, July 2015.
[36] N. Pathak, K. Bandyopadhyay, M. Sarangi and S. Panda, "Microstructure and Mechanical Performance of Friction Stir Spot-Welded Aluminum-5754 Sheets", Journal of Materials Engineering and Performance, Vol. 22, No. 1, pp. 131-144, 2012.
[37] S. Venukumar, S. Yalagi and S. Muthukumaran, "Comparison of microstructure and mechanical properties of conventional and refilled friction stir spot welds in AA 6061-T6 using filler plate", Transactions of Nonferrous Metals Society of China, Vol. 23, No. 10, pp. 2833-2842, 2013.
[38] Z. Shen, X. Yang, Z. Zhang, L. Cui and Y. Yin, "Mechanical properties and failure mechanisms of friction stir spot welds of AA 6061-T4 sheets", Materials and Design, Vol. 49, pp. 181–191, 2013.
[39] T. Rosendo, B. Parra, M. Tier, A. da Silva, J. Santos, T. Strohaecker and N. Alcântara, "Mechanical and microstructural investigation of friction spot welded AA6181-T4 aluminum alloy", Materials & Design, Vol. 32, No. 3, pp. 1094-1100, 2011.
[40] Y. Sun, H. Fujii, N. Takaki and Y. Okitsu, "Novel spot friction stir welding of 6061 and 5052 Al alloys", Science and Technology of Welding and Joining, Vol. 16, No. 7, pp. 605-612, 2011.
[41] H. Badarinarayan, Q. Yang and S. Zhu, "Effect of tool geometry on static strength of friction stir spot-welded aluminum alloy", International Journal of Machine Tools and Manufacture, Vol. 49, No. 2, pp. 142-148, 2009.
[42] S. Hirasawa, H. Badarinarayan, K. Okamoto, T. Tomimura and T. Kawanami, "Analysis of effect of tool geometry on plastic flow during friction stir spot welding using particle method", Journal of Materials Processing Technology, Vol. 210, No. 11, pp. 1455-1463, 2010.
[43] S. Babu, V. Sankar, G. J. Ram, P. Venkitakrishnan, G. M. Reddy and K. Rao, "Microstructures and Mechanical Properties of Friction Stir Spot Welded Aluminum Alloy AA2014", Journal of Materials Engineering and Performance, Vol. 22, No. 1, pp. 71-84, 2013.
[44] Z. Li, S. Gao, S. Ji, Y. Yue and P. Chai, "Effect of Rotational Speed on Microstructure and Mechanical Properties of Refill Friction Stir Spot Welded 2024 Al Alloy", Journal of Materials Engineering and Performance, Vol. 25, No. 4, pp. 1673-1682, 2016.
[45] Z. Shen, Y. Chen, J. Hou, X. Yang and A. Gerlich, "Influence of processing parameters on microstructure and mechanical performance of refill friction stir spot welded 7075-T6 aluminum alloy", Science and Technology of Welding and Joining, Vol. 20, No. 1, pp. 48-57, 2015.
[46] D. Rodrigues, A. Loureiro, C. Leitao, R. Leal, B. Chaparro and P. Vilaça, "Influence of friction stir welding parameters on the microstructural and mechanical properties of AA 6016-T4 thin welds", Materials & Design, Vol. 30, No. 6, pp. 1913-1921, 2009.
[47] M. Fujimoto, S. Koga, N. Abe, Y. Sato and H. Kokawa, "Microstructural analysis of stir zone of Al alloy produced by friction stir spot welding", Science and Technology of Welding and Joining, Vol. 13, No. 7, pp. 663-670, 2008.
[48] F. Gemme, Y. Verreman, L. Dubourg and P. Wanjara, "Effect of welding parameters on microstructure and mechanical properties of AA7075-T6 friction stir welded joints", Fatigue & Fracture of Engineering Materials & Structures, Vol. 34, No. 11, pp. 877-886, 2011.
[49] S. Venukumar, S. Muthukumaran and Y. Swaroop, "Microstructure and Mechanical Properties of Refilled Friction Stir Spot Welding of Commercial Pure Aluminum", Materials Science Forum, Vol. 765, pp. 776-780, 2013.